Correction

MICROBIOLOGY

Correction for "Selective translation by alternative bacterial ribosomes," by Yu-Xiang Chen, Zhi-yu Xu, Xueliang Ge, Suparna Sanyal, Zhi John Lu, and Babak Javid, which was first published July 28, 2020; 10.1073/pnas.2009607117 (*Proc. Natl. Acad. Sci. U.S.A.* **117**, 19487–19496).

The authors note that Jia-Yao Hong should be added to the author list between Xueliang Ge and Suparna Sanyal. Jia-Yao Hong should be credited with performing research. The corrected author line, affiliation line, and author contributions appear below. The online version has been corrected.

Yu-Xiang Chen[a,b], Zhi-yu Xu[a,c], Xueliang Ge[d], Jia-Yao Hong[a], Suparna Sanyal[d], Zhi John Lu[c], and Babak Javid[a,b,e]

[a]Centre for Global Health and Infectious Diseases, Collaborative Innovation Centre for the Diagnosis and Treatment of Infectious Diseases, Tsinghua University School of Medicine, 100084 Beijing, China; [b]Division of Experimental Medicine, University of California, San Francisco, CA 94110; [c]Ministry of Education Key Laboratory of Bioinformatics, Center for Synthetic and Systems Biology, School of Life Sciences, Tsinghua University, 100084 Beijing, China; [d]Department of Cell and Molecular Biology, Uppsala University, 75124 Uppsala, Sweden; and [e]Beijing Advanced Innovation Center in Structural Biology, 100084 Beijing, China

Author contributions: Y.-X.C. and B.J. designed research; Y.-X.C., X.G., and J.-Y.H. performed research; Y.-X.C. and Z.-y.X. contributed new reagents/analytic tools; Y.-X.C., Z.-y.X., S.S., Z.J.L., and B.J. analyzed data; and Y.-X.C. and B.J. wrote the paper.

www.pnas.org/cgi/doi/10.1073/pnas.2017631117

Selective translation by alternative bacterial ribosomes

Yu-Xiang Chen[a,b,1], Zhi-yu Xu[a,c,1], Xueliang Ge[d], Jia-Yao Hong[a], Suparna Sanyal[d], Zhi John Lu[c,2], and Babak Javid[a,b,e,2]

[a]Centre for Global Health and Infectious Diseases, Collaborative Innovation Centre for the Diagnosis and Treatment of Infectious Diseases, Tsinghua University School of Medicine, 100084 Beijing, China; [b]Division of Experimental Medicine, University of California, San Francisco, CA 94110; [c]Ministry of Education Key Laboratory of Bioinformatics, Center for Synthetic and Systems Biology, School of Life Sciences, Tsinghua University, 100084 Beijing, China; [d]Department of Cell and Molecular Biology, Uppsala University, 75124 Uppsala, Sweden; and [e]Beijing Advanced Innovation Center in Structural Biology, 100084 Beijing, China

Edited by Ralph R. Isberg, Tufts University School of Medicine, Boston, MA, and approved June 29, 2020 (received for review May 15, 2020)

Alternative ribosome subunit proteins are prevalent in the genomes of diverse bacterial species, but their functional significance is controversial. Attempts to study microbial ribosomal heterogeneity have mostly relied on comparing wild-type strains with mutants in which subunits have been deleted, but this approach does not allow direct comparison of alternate ribosome isoforms isolated from identical cellular contexts. Here, by simultaneously purifying canonical and alternative RpsR ribosomes from *Mycobacterium smegmatis*, we show that alternative ribosomes have distinct translational features compared with their canonical counterparts. Both alternative and canonical ribosomes actively take part in protein synthesis, although they translate a subset of genes with differential efficiency as measured by ribosome profiling. We also show that alternative ribosomes have a relative defect in initiation complex formation. Furthermore, a strain of *M. smegmatis* in which the alternative ribosome protein operon is deleted grows poorly in iron-depleted medium, uncovering a role for alternative ribosomes in iron homeostasis. Our work confirms the distinct and nonredundant contribution of alternative bacterial ribosomes for adaptation to hostile environments.

mycobacterium | alternative ribosomes | ribosome profiling

Ribosomes are the macromolecular machines that translate the genetic code into functional proteins (1–3). Shortly after their discovery and role in gene translation, the "one gene, one messenger RNA (mRNA), one ribosome" hypothesis was proposed (4), but was quickly disproven (5). This led, in turn, to the "homogeneity hypothesis" for ribosomes: that all ribosomes were identical macromolecules, that would translate all mRNAs with equal efficiency (6). However, observations that ribosome composition varied according to environmental conditions and other variables immediately challenged the homogeneity hypothesis (7). But, until recently, the functional significance of ribosome heterogeneity has not been well understood.

In eukaryotic systems, there is increasing evidence for the role and importance of ribosomal heterogeneity in fundamental physiology, development, and disease, in systems from budding yeast to organelles and animals (8–11). In particular, studies have suggested, not entirely without controversy (12, 13), that specialized ribosomes are important for vitamin B12 transport and cell cycle components (14), hematopoiesis (15), and development (16). Mutations in ribosomal proteins, or haploinsufficiency of their coded genes, have been implicated in a number of disorders such as the ribosomopathies (9, 17). Our understanding of ribosomal heterogeneity in bacteria is less advanced (18). High-fidelity mass spectrometry of intact 70S ribosomes from *Escherichia coli* revealed considerable heterogeneity, such as the presence or absence of the stationary-phase-induced ribosomal-associated protein, SRA (19). Other studies implicating specialized bacterial ribosomes (20, 21) have recently been questioned (22–25). Nonetheless, it is intriguing to speculate that alternative bacterial ribosomes, generated in response to environmental stressors, would result in altered translation, which, in turn, might allow adaptation to the stressful environment (18, 26, 27).

Alternative ribosomes could be generated via changes in the stoichiometry of canonical ribosomal components, association of accessory ribosomal proteins, modification of ribosomal RNA (rRNA), or incorporation of alternative ribosomal subunits, coded by paralogous or homologous genes (reviewed in refs. 9, 28, and 29). Most eukaryotic organisms code for paralogues of ribosomal subunit genes, and around half of sequenced bacterial genomes from one study included at least one ribosomal protein paralogue (30). One well-characterized group of paralogous ribosomal proteins are those that lack cysteine-rich motifs (C−) compared with canonical cysteine-containing homologs (C+). C− paralogues have been described in many bacteria, including mycobacteria (31–33). In mycobacteria, the conserved alternative C− ribosomal subunits are coded in a single operon regulated by a zinc uptake regulator (zur), which represses expression in the presence of zinc ions (34), and has led to the suggestion that the function for C−/C+ ribosomal subunit paralogues is to allow for dynamic storage of zinc (35–37). Furthermore, although these alternative mycobacterial ribosomal proteins (AltRPs) have recently been demonstrated to incorporate into assembled ribosomes, it has been suggested that they form nontranslating hibernating ribosome complexes due to exclusive

Significance

Many organisms, including bacteria, code for multiple paralogues of some ribosomal protein subunits. The relative contribution of these alternative subunits to ribosome function and protein synthesis is unknown and controversial. Many studies on alternative ribosomes have been confounded by isolation of alternative and canonical ribosomes from different strains or growth conditions, potentially confounding results. Here, we show that one form of alternative ribosome from *Mycobacterium smegmatis* has a distinct translational profile compared with canonical ribosomes purified from an identical cellular context. We also identify a role for alternative ribosomes in iron homeostasis. Given the prevalence of alternative ribosomal genes in diverse organisms, our study suggests that alternative ribosomes may represent a further layer of regulation of gene translation.

Author contributions: Y.-X.C. and B.J. designed research; Y.-X.C., X.G., and J.-Y.H. performed research; Y.-X.C. and Z.-y.X. contributed new reagents/analytic tools; Y.-X.C., Z.-y.X., S.S., Z.J.L., and B.J. analyzed data; and Y.-X.C. and B.J. wrote the paper.

The authors declare no competing interest.

This article is a PNAS Direct Submission.

Data deposition: Ribosome profiling and RNAseq data have been deposited in in the Gene Expression Omnibus (GEO) database, https://www.ncbi.nlm.nih.gov/geo (accession no. GSE127827).

[1]Y.-X.C. and Z.-y.X. contributed equally to this work.

[2]To whom correspondence may be addressed. Email: zhilu@tsinghua.edu.cn or bjavid@gmail.com.

This article contains supporting information online at https://www.pnas.org/lookup/suppl/doi:10.1073/pnas.2009607117/-/DCSupplemental.

First published July 28, 2020.

association of a hibernation factor with alternative ribosomes (38). Here, we demonstrate, using a fully reconstituted mycobacterial translation system, that ribosomes containing the alternative subunit RpsR2 (AltRpsR) actively translate. Furthermore, the translational landscapes as measured by ribosome profiling of these alternative mycobacterial ribosomes are distinct from those generated by canonical ribosomes purified from the same cell and are characterized by a 5′ positional polarity shift. Alternative ribosome proteins were also necessary for optimal growth in iron-depleted medium, suggesting that alternative bacterial ribosomes may provide a further layer of regulation during nutrient stress.

Results

Alternative Mycobacterial Ribosomes Engage in Gene Translation. Mycobacteria encode for several alternative C– ribosomal proteins, four of which are conserved throughout the genus and are encoded within one operon (32, 38) (Fig. 1 *A* and *B*). We wished to biochemically characterize alternative ribosome (AltRibo) function by purifying ribosomes containing alternative or canonical subunit proteins. We chose to C-terminally tag RpsR2 (AltRpsR) with 3xFLAG, since, of the four alternative ribosome genes within the operon, the C terminus of RpsR showed the greatest sequence variation, and we reasoned that it therefore was most likely to tolerate tagging.

To investigate alternative (AltRibo) and canonical (CanRibo) RpsR ribosome function within the same cellular context, we constructed a strain of *Mycobacterium smegmatis* in which both RpsR subunits had affinity tags inserted at their C terminus, at their native loci on the mycobacterial chromosome (Fig. 1*B* and see *Materials and Methods*). In keeping with prior studies (33, 39), growth of mycobacteria in relatively zinc-depleted Sauton's medium up-regulated AltRpSR expression, and supplementation with zinc restored CanRpsR expression (*SI Appendix*, Fig. S1*A*). To investigate whether tagged AltRibo and CanRibo pull-down would be able to isolate intact ribosomes, we subjected immunoprecipitated ribosomes to semiquantitative mass spectrometry with labeling by tandem mass tags (TMT; *SI Appendix*, Fig. S2*A*). Of note is that our purification strategy was able to isolate ribosomes including all ribosomal subunits. AltRibos were four-fold enriched for AltRpsR (RpS18), but not the other alternative ribosomal subunits to a similar degree (*SI Appendix*, Fig. S2 and Dataset S1). The AltRibos also enriched for other, non-ARP rProteins, for example, S19 (*SI Appendix*, Fig. S2); therefore, the alternative ribosomes studied by our tagging strategy under these growth conditions represent RpsR AltRibos.

We grew the dual-tagged *M. smegmatis* strain in both zinc-replete and relatively zinc-depleted conditions, purified ribosomes, and subjected them to subunit profiling. Under both conditions, translating ribosomes (polysome fraction) could clearly be identified (Fig. 1*C*). Immunoblotting against AltRpsR-FLAG and CanRpsR-HA confirmed that zinc depletion up-regulated AltRpsR expression. Importantly, a substantial proportion of polysomes isolated from growth in zinc-depleted medium were AltRibos (Fig. 1*C*), suggesting that AltRibos are resident on translating polysomes and supporting their active role in gene translation. We further subjected affinity purified AltRibos and CanRibos to biochemical analysis in a mycobacterial cell-free translation system (39). AltRibos were able to synthesize dipeptides at an efficiency similar to CanRibos (Fig. 1*D*), confirming that AltRibos are capable of protein synthesis.

We also constructed a strain in which the alternative subunit operon was knocked out, ΔARP. This strain grew poorly with medium in which zinc was depleted by N,N,N,N′-tetrakis (2-pyridinylmethyl)-1,2-ethanediamine (TPEN) (*SI Appendix*, Fig. S3), confirming prior results. We wondered whether this might be because, under conditions of zinc depletion, CanRibos are less proficient at protein synthesis. We performed subunit profiling on both wild-type and ΔARP *M. smegmatis*, scraped both from agar plates grown on standard medium (7H10-agar) and plates supplemented with TPEN at a concentration of TPEN that did not interfere with bacterial growth (*SI Appendix*, Fig. S4). Although the polysome fraction was preserved in both strains when isolated from standard growth conditions, the polysome fraction of ΔARP was substantially smaller under zinc depletion (Fig. 1*E*), suggesting that canonical ribosomes may translate less effectively under zinc depletion, and that alternative RpsR ribosomes are likely to be the major translating fraction under those conditions.

Alternative Mycobacterial Ribosomes Have Distinct Translational Profiles Compared with Canonical Ribosomes. The dual-RpsR-tagged strain (strain A) permitted us to interrogate selective ribosome translation profiles from the same cellular population, which would eliminate potential differences due to mRNA abundance or other confounding factors (40, 41). We grew the strains in relatively zinc-replete conditions, which allowed cultures to grow to greater density for ribosome isolation prior to ribosome profiling (40, 42–44). Under these conditions, the majority of ribosomes were CanRibos. To exclude the formal possibility that observed differences were due to the use of the affinity tags, we generated a second dual-tagged strain in which the affinity tags were swapped (strain B, Fig. 2*A*). Both strains were similarly regulated by zinc (32, 38) (*SI Appendix*, Fig. S1), suggesting they had comparable physiology.

Position analysis of aligned reads revealed a clear three-nucleotide periodicity (*SI Appendix*, Fig. S5), confirming that reads were derived from translating ribosomes for both AltRibos and CanRibos, and showed a high degree of reproducibility between replicates (*SI Appendix*, Table S1). Comparison of translational profiles confirmed that CanRibo-derived reads were highly correlated with total ribosome input, consistent with the fact that the majority of ribosomes under the tested condition were CanRibos (*SI Appendix*, Fig. S6). However, reads generated from AltRibos were less well correlated, suggesting that translational profiles from AltRibos were distinct from CanRibos (Fig. 2*B*). Regardless of affinity tag, CanRibo- and AltRibo-derived reads were highly correlated with themselves when comparing translational efficiency profiles generated by strain A and strain B (Fig. 2*C*), following correction for mRNA expression (*SI Appendix*, Table S1). These data, together, strongly support that AltRibos and CanRibos generate distinct translational landscapes.

Our data suggested that alternative ribosomes had intrinsic differences in gene translation compared with canonical ribosomes. We performed differential expression analysis on AltRibo- and CanRibo-generated ribosome profile datasets, and compared these with the total ribosome input. Pull-down efficiency (but not purity) of HA-tagged subunits was less efficient than FLAG-tagged subunits. Although this was not an issue in strain A, where the highly abundant CanRibos were HA tagged, it meant that the number of reads from the HA-tagged AltRibos from strain B were lower, and, as such, fewer genes were differentially translated (up or down) in AltRibos isolated from strain B. As expected, there were few differences between CanRibos and total ribosomes. By contrast, there were a large number of genes that were translated with either decreased or increased preference by AltRibos compared with total ribosome input (Fig. 2 *D* and *E* and Dataset S2). Of note is that there was significantly greater enrichment in underrepresented translated genes in AltRibos isolated from strains A and B (*SI Appendix*, Fig. S7). Gene ontology analysis of the overrepresented and underrepresented translated genes revealed overlap between strain A and strain B in membrane proteins and growth-related proteins for underrepresented genes (Fig. 2*F*), but no overlap for enriched genes (*SI Appendix*, Fig. S7*B*).

Alternative Ribosomes Have Positional Polarized Read Distribution and a Relative Initiation Defect. Our analysis of differences in translational profiles between canonical and alternative mycobacterial

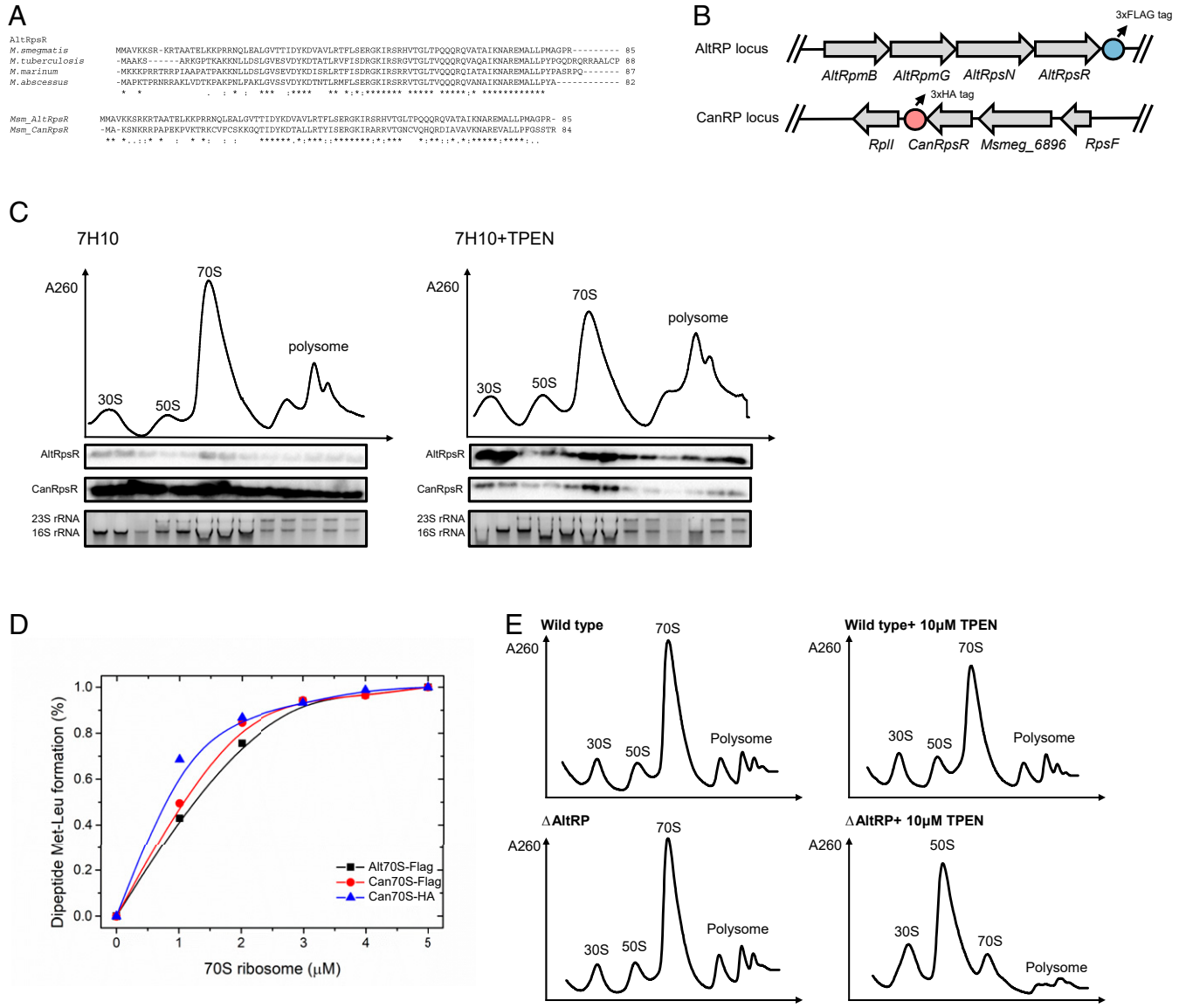

Fig. 1. Alternative mycobacterial ribosomes engage in protein synthesis, even in zinc depletion. (*A*) (*Upper*) Sequence alignments of AltRpsR from 4 mycobacterial species. (*Lower*) Sequence alignments of the AltRpsR and CanRpsR in *M. smegmatis*. (*B*) Cartoon representing the C terminus affinity tagging of the CanRpsR and AltRpsR native loci. (*C*) Ribosome subunit profiling of strain A (depicted in *B*) ribosomes purified from either 7H10-agar or 7H10-agar + 10 μM TPEN plates. The corresponding 30S, 50S, 70S, and polysome fractions are indicated. Each fraction was blotted with anti-FLAG and anti-HA antibodies. The 16S and 23S rRNA of each fraction are shown as loading control. Results are representative of three independent experiments. (*D*) Dipeptide formation of AltRibos vs. CanRibos with a fully reconstituted mycobacterial translation system (38). Peptides were detected and analyzed by HPLC. (*E*) Ribosome subunit profiling of wild-type *M. smegmatis* and the ΔAltRP strain purified from 7H10 agar plate ± 10 μM TPEN. The corresponding 30S, 50S, 70S, and polysome fractions are indicated. Results are representative of two experiments.

ribosomes revealed that, for translation of certain genes, there were clear differences in the distribution of sequencing reads along the gene length between the two samples, for example, for translation of *Msmeg_0363* (Fig. 3*A*). To characterize these differences on a genome-wide basis, we calculated the polarity score to determine the distribution of aligned reads for each coding gene (45). Polarity scores between −1 and 0 represent read accumulation at the 5′ end of the coding region, and scores between 0 and +1 represent read accumulation at the 3′ end of the coding region (see *Materials and Methods*). Comparing the polarity score of AltRibos with CanRibos and total ribosome input from both strain A and strain B, there was a clear positional polarity shift toward a 5′ read accumulation in alternative ribosomes (Fig. 3*B*).

Translation elongation does not proceed at a uniform pace (46–48). We investigated whether alternative and canonical ribosomes differed in codon occupancy. AltRibos from either strain A or strain B showed similar, although not identical, codon occupancy patterns across all 61 sense codons (Fig. 3*C* and *SI Appendix*, Fig. S8*A*). Comparing CanRibos with AltRibos with total ribosome input across all coding genes, there were significant differences in codon occupancy between the two ribosome isoforms in both strain A and strain B (Fig. 3*D* and *SI Appendix*, Fig. S8*B*). From our analysis of all 61 sense codons in both strains, 12 showed relatively high occupancy in AltRibos compared with total ribosomes, and 12 showed relatively low occupancy (*SI Appendix*, Fig. S8*C*). We wished to determine whether altered codon occupancy might be associated with the observed

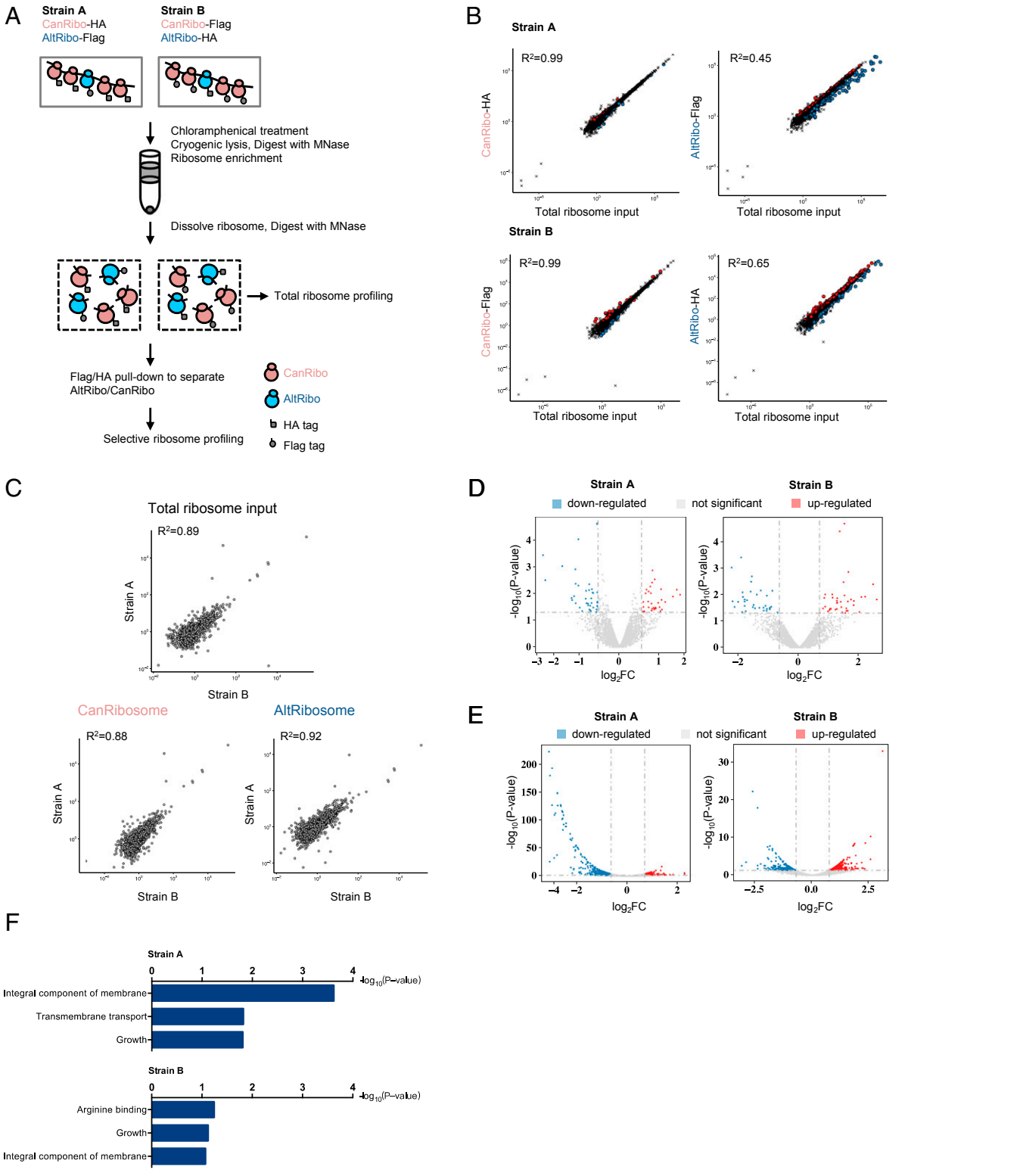

Fig. 2. Alternative ribosomes have distinct translational profiles. (*A*) Cartoon outlining work flow for performing selective ribosome profiling in the two RpsR-tagged strains—strain A and strain B (and see *Materials and Methods*). (*B*) Scatter plot showing selective ribosome profiles compared with total ribosome input in strain A and strain B. Axes represent RPKM. Blue and red dots represent down- and up-regulated reads, respectively. R^2 represents Pearson correlation. (*C*) Correlation of translation efficiency of total ribosome, selective CanRibo, and selective AltRibo inputs in strain A compared with strain B. R^2 represents Pearson correlation. (*D* and *E*) Normalized ribosome profile read density for (*D*) CanRibos and (*E*) AltRibos compared with total ribosome input in strain A and strain B. Significantly up-regulated (log2 FC > 0.5, *P* value < 0.05) and down-regulated (log2 FC < −0.5, *P* value < 0.05) genes are represented by red and blue dots, respectively. (*F*) Gene ontology analysis (using DavidTools) of the top three categories of down AltRibo-enriched translated genes.

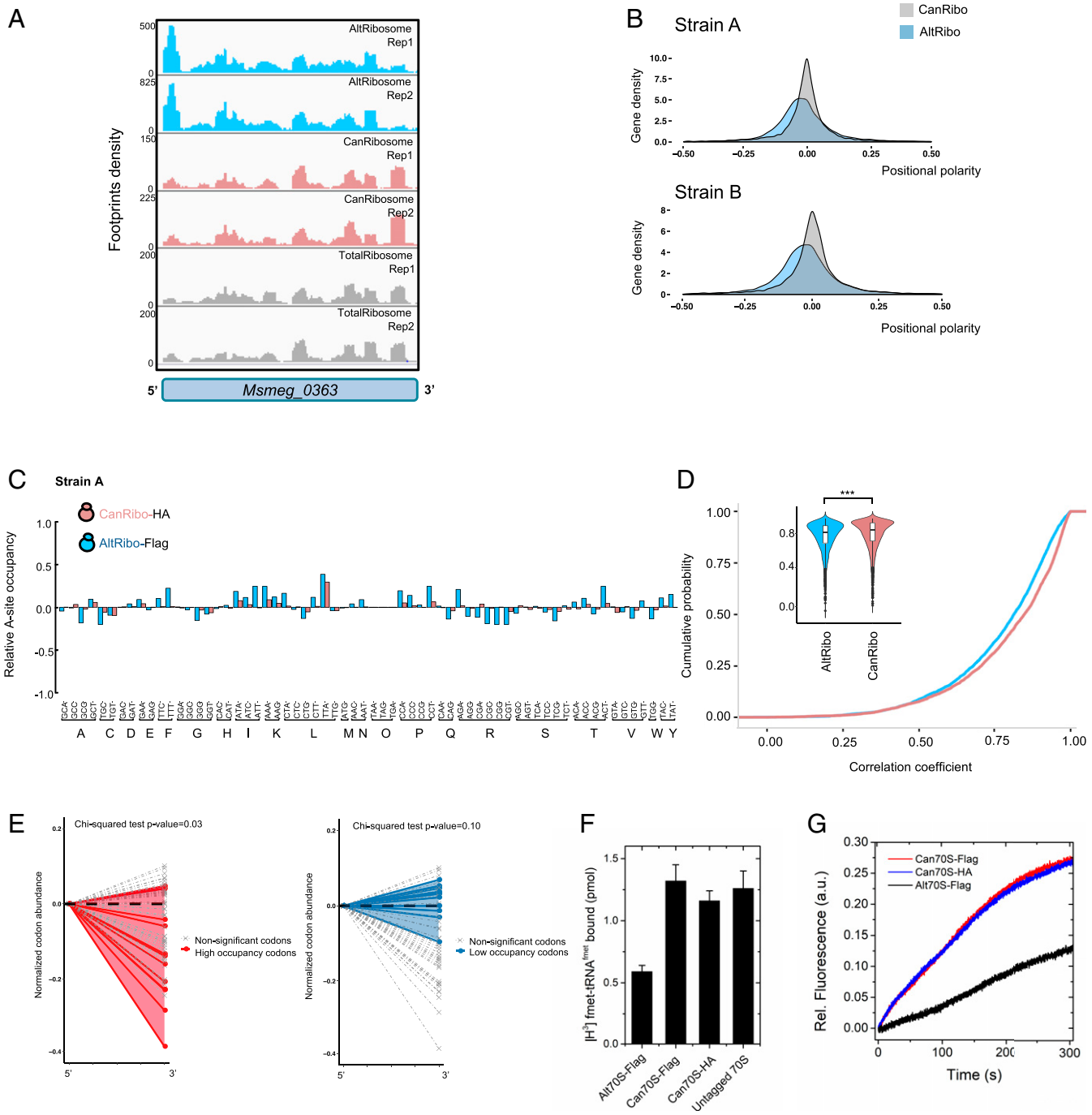

Fig. 3. Alternative ribosomes have 5′ read accumulation and a relative initiation defect compared with canonical ribosomes. (*A*) Normalized reads of each ribosome input for the gene Msmeg_0363 were plotted along gene length using IGV software (see *Materials and Methods*). Reads from AltRibos show a clear 5′ accumulation compared with reads generated from CanRibos or total ribosomal input. (*B*) Shifts in positional polarity scores for the entire genome generated from selective AltRibo and CanRibo reads from strains (*Upper*) A and (*Lower*) B. A negative score indicates 5′ read accumulation, and a positive score indicates a 3′ read accumulation. (*C*) The relative A-site codon occupancy for all 61 sense codons for AltRibos and CanRibos in strain A compared with total ribosome input. (*D*) Cumulative probability and violin (*Inset*) plots for correlation of each gene between codon occupancy for AltRibos and CanRibos compared with total ribosome input from strain A. ***$P < 0.001$ by Student's t test. (*E*) The relative codon frequencies of the 5′ 50 codons and 3′ 50 codons for each ORF were analyzed. Comparing AltRibo (*Left*) high-occupancy codons and (*Right*) low-occupancy codons with nonsignificantly enriched codons, there was significant enrichment of high-occupancy codons at the beginning of ORFs, and a trend toward enrichment of low-occupancy codons at the end of ORFs, by χ^2 test. (*F*) The extent of initiation complex formation by AltRibos compared with CanRibos measured by retention of 3H-fMet count on a nitrocellulose filter. (*G*) The kinetics and extent of binding of the initiator tRNA to the mRNA programmed 70S ribosome (AltRibo vs. CanRibo) followed with boron-dipyrromethene (BODIPY) fluorescence.

polarity differences between AltRibos and CanRibos. We considered the first and last 50 codons of all coding genes and compared the relative abundance of the 12 high- and 12 low-occupancy codons in these regions. For the 12 high-occupancy codons, 10 were relatively enriched at the 5′ end of coding regions, and for the 12 low-occupancy codons, 8 were relatively enriched at the 3′ end of coding regions (Fig. 3*E*). Furthermore, although purified AltRibos formed 70S initiation complexes, they appeared to do so at slightly lower efficiency compared with CanRibos (Fig. 3*F*), suggesting another potential mechanism for the observed 5′ polarity shift. The lower efficiency in 70S initiation complex formation could be due to impaired binding of the initiator transfer RNA (tRNA) as demonstrated by BODIPY-Met-tRNA^{fMet} binding to the ribosome monitored by increase in BODIPY fluorescence (Fig. 3*G*).

Our in vivo and in vitro data suggested that, although AltRibos and CanRibos both partake in protein synthesis, they are not identical in translation. Both our observed positional polarity shift from ribosome profiling and our biochemical data suggested that AltRibos may have a relative initiation defect. Given the potential role of AltRibos for protein synthesis under zinc-depleted conditions, which may be a marker of generalized environmental stress, could it be that AltRibos are "slow and accurate" compared with CanRibos? To address relative translation rates, we made a modified Nluc luciferase reporter under control of a tetracycline promoter, in which the C terminus was tagged to make the translated protein unstable (ref. 49 and *SI Appendix*, Fig. S9*A*, and see *Materials and Methods*). This would ensure that measured Nluc activity represented recently synthesized proteins following addition of the ATc inducer, and not due to accumulation of the luciferase prior to induction by ATc due to leaky expression from the promoter. Measurement of Nluc activity after a 5-min pulse under conditions of normal zinc (CanRibo dominant) and zinc depletion with TPEN (AltRibo dominant) did not reveal any differences (*SI Appendix*, Fig. S9*B*), suggesting that protein synthesis rates under conditions that favor either CanRibos or AltRibos do not measurably differ. Addition of chloramphenicol as a protein synthesis inhibitor to examine Nluc synthesized only during the pulse and not subsequently also confirmed the same result. We also looked for correlations of codon usage frequency and AltRibo and CanRibo translatomes and did not find any consistent patterns that might suggest that AltRibo codon occupancy is associated with rare codons or vice versa (*SI Appendix*, Figs. S10 and S11).

RpsR (S18) has been implicated in accuracy of translational decoding due to a potential role in constraining mRNA exit from the ribosome (50). We measured relative translational error rates in high/low zinc conditions using three different reporters that measure ribosomal decoding errors (51–53). Again, there were no significantly different rates of translational error (*SI Appendix*, Fig. S12), suggesting that AltRibos are neither more nor less accurate than CanRibos in decoding mRNA, and can equally well translate a model protein.

To gain further potential insights into AltRibo function, we examined the relative enrichment of "ribosome-associated" proteins (41) that were pulled down with either the AltRibos or CanRibos in our semiquantitative mass spectrometry analysis (Dataset S1). There were several proteins that were enriched with either AltRibos or CanRibos (Fig. 4*A*). Of note is that two of the top three AltRibo-enriched proteins were type VII secretion-associated proteins. Furthermore, we only isolated two Esx-3-associated proteins (EccB3 and EccC3), both of which were relatively AltRibo enriched (Fig. 4*A*). Since Esx-3 has been implicated in iron homeostasis in mycobacteria (54), and, furthermore, is, similarly to ARPs, regulated by the *zur* regulon (55), we wondered whether AltRibos might play a role under iron depletion conditions. We therefore compared growth of wild-type *M. smegmatis*, the ΔAltRP strain, and ΔAltRP complemented with the AltRP operon in medium that had iron removed by chelex 100 (54). In iron-chelated medium, ΔAltRP had a major growth defect. Since chelex 100 is a relatively nonspecific metal chelator, we supplemented medium with either zinc or iron. Zinc supplementation led to only partial rescue, but the growth defect could only be fully complemented by replacement of either the operon or iron (Fig. 4*B*), suggesting a specific iron-limiting phenotype for mycobacteria lacking the alternative ribosome operon.

Discussion

Together, our studies demonstrate that alternative mycobacterial ribosomes incorporating the C– paralogue AltRpsR are not only competent for translation but that these alternative ribosomes have distinct translational landscapes compared with their canonical counterparts. The ribosome is an RNA machine (2), and recent studies have identified functional importance for rRNA heterogeneity in bacterial ribosomes (26, 27, 56). The role of rProtein heterogeneity is more controversial, but multiple studies have shown that alterations, for example, by mutation, in ribosomal subunit proteins may also have profound impacts on aspects of translation function (14, 41, 57, 58). Furthermore, since RpsR forms part of the 30S "core" that interacts directly with 16S rRNA (59), it is possible that ribosomes composed of alternate RpsR isoforms may influence diverse aspects of ribosome function.

We leveraged the power of ribosome profiling and affinity purification of alternative ribosomes to show that alternative RpsR mycobacterial ribosomes have altered codon occupancy compared with ribosomes containing the canonical RpsR paralogue, as well as a relative 5′ positional polarity shift in translation of open reading frames (ORFs). It should be noted that, due to our tagging and purification strategy, we were primarily comparing RpsR canonical and alternative ribosomes. Due to their differential expression, we would expect that, in

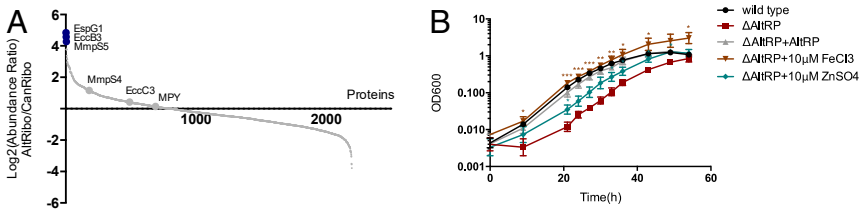

Fig. 4. Mycobacterial AltRPs are required for optimal growth in iron depletion. (*A*) Log_2 FC of protein abundance of AltRibo/CanRibo of each protein candidate from semiquantitative mass spectrometry analysis. Top three protein interactions with AltRibo (in blue) as well as MmpS4, EccC3, and MPY are highlighted. (*B*) Growth curve (as measured by OD_{600nm}) in chelated medium for wild-type *M. smegmatis*, *M. smegmatis*-ΔAltRP (ΔAltRP), *M. smegmatis*-ΔAltRP complemented with the AltRP operon (ΔAltRP + AltRP), or *M. smegmatis*-ΔAltRP (ΔAltRP) grown in chelated medium subsequently supplemented with iron (ΔAltRP + 10 μM $FeCl_3$) or zinc (ΔAltRP + 10 μM $ZnSO_4$). Data show biological triplicates ± SD, and results are representative of two independent experiments. $^*P < 0.05$, $^{**}P < 0.01$, $^{***}P < 0.001$ by Student's *t* test. Brown asterisks represent comparison between ΔAltRP and ΔAltRP + 10 μM $FeCl_3$; green asterisks represent comparison between ΔAltRP and ΔAltRP + 10 μM $ZnSO_4$.

high and low zinc environments, alternative and canonical ribosomes would contain mostly the entire canonical or alternative subunit proteins. In environments where expression of all subunits is sustained (such as our experimental conditions), multiple combinations of "alternative" ribosomes could coexist, and our data are unable to resolve between these. Ribosomal profiling of specialized ribosomes had previously demonstrated specific functions of heterogeneous ribosome populations in stem cells and for the translation of mitochondrial proteins in eukaryotic cells (14, 57). In bacteria, ribosome profiling of trigger factor associated with ribosomes demonstrated the requirement of trigger factor particularly for the translation of outer membrane proteins in *E. coli* (41), but ribosome profiling had not been employed for ribosomes incorporating ribosomal protein paralogues.

There have been relatively few studies of bacterial ribosomal heterogeneity when compared with eukaryotic systems (18). However, there is evidence that ribosomal heterogeneity may be just as pervasive in bacteria as eukaryotes (26, 27, 56). Mycobacteria, for example, have very distinct translational features compared with the model *E. coli* system (44, 60, 61). Recent structural information about the mycobacterial ribosome identified new ribosomal protein subunits, but these new subunits, bL37 and bS22, were not present in all ribosomes identified by cryoelectron microscopy (39, 62, 63).

Many diverse bacterial species code for C− ribosomal subunit paralogues (30), but their distinct translational functions, if any, have not been fully characterized. A recent examination of the mycobacterial C− paralogues that are the subject of this study suggested that C− ribosomes are hibernating and do not actively engage in gene translation under zinc depletion due to exclusive C− ribosome interaction with the hibernation factor MPY (38, 64). Those findings are in contradistinction with our own. By both biochemical analysis and ribosome profiling, our data support a role for translating AltRibos, even under conditions of zinc depletion. It is possible that use of supraphysiological (1 mM) zinc in culture medium—50 times higher than the concentrations in human plasma (65)—led to lack of binding of MPY to canonical (C+) ribosomes under those conditions (38). However, our isolation of ribosomes from standard growth medium showed lack of enrichment of MPY with AltRibos compared with CanRibos (Fig. 4*A*). We also demonstrated that canonical ribosomes are less competent at polysome formation under zinc depletion (Fig. 1*E*). Together with previous studies of *M. smegmatis* grown under conditions where C− ribosomes would not have been predominant (66, 67), these data suggest that MPY is not exclusively associated with C− ribosomes.

Structural data showed association of aminoacylated tRNA with C− ribosomes (33), supporting a role for C− ribosomes in protein synthesis. However, our data suggest that alternative ribosomes and canonical ribosomes are not only competent for protein synthesis, but they have differences potentially in both translation initiation and codon occupancy. Both of these differences may contribute to the relative 5′ positional polarity shift of reads in alternative ribosomes as well as the specific enrichment only of down-regulated synthesized proteins by AltRibos. However, we cannot exclude that the positional polarity itself led to the codon occupancy differences observed in the beginning and end of genes (Fig. 3*E*). Multiple mechanisms have been proposed for observed differences in codon occupancy and elongation (68). Decoding of modified tRNA bases (47) and differential affinity of specific ribosome isoforms for aminoacyl tRNAs (46) also contribute to altered rates of gene translation. Of note is that RpS18 (of which AltRpsR and CanRpsR are the two mycobacterial isoforms) is part of an mRNA "nest," which contributes to preinitiation binding of mRNA to the 30S subunit (69), and it is tempting, therefore, to speculate that differences in RpsR protein sequence may contribute the observed differences in initiation complex formation.

We have also uncovered a role for the alternative ribosome operon in iron homeostasis: Mycobacteria lacking this operon have substantially attenuated growth under iron limitation compared with wild-type *M. smegmatis*. This was not entirely due to nonspecific chelation of zinc by chelex-100. Supplementation of zinc led to only partial rescue of the growth defect, unlike the full complementation seen with iron supplementation alone. While the precise molecular mechanisms by which AltRPs contribute to iron homeostasis is unknown, we were intrigued by the observation that pull-down of AltRibos enriched for interactions with *esx-3*, as well as siderophore synthesis-associated proteins (Fig. 4*A*). The recent finding that *M. smegmatis* ΔARP had a pronounced colony morphology phenotype (70) suggest that ARPs may be implicated in the maintenance of the mycobacterial membrane and secretion apparatus. Our study confirms not only that alternative mycobacterial ribosomes actively participate in protein synthesis but also that RpsR alternative ribosomes have distinct translational features, and alternative bacterial ribosomes contribute to environmental adaptation.

Materials and Methods

Bacterial Strains and Culture. Wild-type *M. smegmatis* mc^2-155 (71) and derived strains were grown in either Middlebrook 7H9 media supplemented with 0.2% glycerol, 0.05% Tween-80, 10% albumin-dextrose-salt with appropriate antibiotics, or Sauton's medium (0.05% KH_2PO_4, 0.05% $MgSO_4 \cdot 7H_2O$, 0.2% citric acid, 0.005% ferric ammonium citrate, 6% glycerol, 0.4% asparagine, 0.05% Tween, pH 7.4) (32). Zinc sulfate at indicated concentrations was added to Sauton's medium as per specific protocols. For the iron depletion experiments, we modified a previous method (54). Briefly, Sauton's medium was prepared as above with the exception of the magnesium sulfate. After preparation, 10 g of chelex 100 resin was added to 1 L of medium, thoroughly mixed, and left for 24 h. The medium was sterile filtered to remove the chelating agent beads, and 1 g of sterile $MgSO_4 \cdot 7H_2O$ was added to the medium. Zinc sulfate and iron chloride were also supplemented at the indicated concentrations as appropriate for the experimental condition. If not otherwise noted, bacteria were grown and maintained at 37 °C with shaking.

***M. smegmatis* AltRP Knock-Out Strain and Complemented Strain Construction.** In normal conditions (High Zinc), the AltRP operon is not required for growth. A double cross-over strategy was used to construct an unmarked AltRP knockout strain as previously described (72). Sequences 1,000 base pairs (bp) upstream and downstream of the operon were cloned and ligated into the P2NIL suicide vector. The lacZ and SacB genes were cloned from pGOAL17 and ligated to P2NIL containing upstream and downstream 1,000-bp regions to generate the AltRP deletion construct. Two micrograms of plasmid were transformed to wild-type *M. smegmatis* competent cells by electrophoresis and selected on lysogeny broth (LB) plates supplemented with 25 μg/mL kanamycin and 50 μg/mL X-gal. Blue colonies were screened for single cross-over recombinants and further verified by PCR. Correctly identified recombinants were further plated on LB plates containing X-gal and 2% sucrose with 10-fold serial dilutions. White colonies were screened for double cross-over strains by PCR verification. A correct knockout strain was further verified by Southern blot and used in subsequent experiments.

For complementation of the knockout strain, the upstream 500 bp of the coding region for the AltRP operon (presumably incorporating the promoter region) along with the whole AltRP operon was cloned with C-terminal 3xFlag tag to AltRpsR and ligated to pML1342 as a complementation plasmid. The plasmid was transformed to ΔAltRP competent cells and plated on LB plates with 50 μg/mL hygromycin. Recombinants were further verified by Western blot in Sauton's medium supplemented with different concentrations of zinc to check the expression from the operon.

Generating Endogenous AltRpsR/CanRpsR with Different Affinity Tags Strains. Upstream 500 bp (US500) and downstream 500 bp (DS500) of AltRpsR/CanRpsR, stop codons were cloned. Different affinity tag sequences (3xFlag/3xHA) fused with different antibiotic expression cassette (Hygromycin/Zeocin) were generated by overlap PCR (3xFlag-Zeo oligo cassette was kindly provided by Jun-Hao Zhu, Harvard University). The upstream, tag, antibiotic, and downstream cassettes were fused by Gibson assembly and cloned into pUC19 vector. The pUC19 plasmid containing four different recombineering oligo cassettes (AltRpsR-3Flag-Zeo, AltRpsR-3HA-Hyg, CanRpsR-3HA-Hyg, and CanRpsR-3Flag-Zeo) was generated. *M. smegmatis* containing the

plasmid pNitET-SacB-kan (73) was grown to optical density at 600 nm (OD_{600nm}) ≈ 0.2, and 10 μM isovaleronitril was added to induce the expression of RecET; after inducing for 6 h, competent cells were prepared by three washes in 10% glycerol. Oligos for recombineering were amplified from pUC19 series plasmid, and 2 μg of DNA were transformed to the competent cells. Bacteria were plated on LB plates supplemented with either 50 μg/mL Hygromycin or 20 μg/mL Zeocin. Desired colonies were genotyped by PCR and further verified by Western blot to test the expression of AltRpsR/CanRpsR by blotting with either Flag or HA antibody respectively.

Western Blot to Test Zinc-Switch Phenotype. Strain A and strain B were cultured in 7H9 medium to stationary phase (OD_{600nm} ≈ 3) and subcultured 1:500 to Sauton's medium (zinc free) supplemented with different concentrations of zinc sulfate. When bacteria reached stationary phase, bacteria were washed and resuspended in TE buffer. The bacterial suspension was disrupted by bead beating and lysate centrifuged at 17,950 × *g*, 4 °C for 5 min. Protein concentration was quantified by Bradford assay (Bio-Rad), and the same amount of protein was loaded onto 5%/12% sodium dodecyl sulfate polyacrylamide gel electrophoresis (SDS/PAGE) gel. Proteins were further transferred onto poly(vinylidene difluoride) membrane (Bio-Rad). The membrane was blocked in 4% skim milk at room temperature (RT) for 1 h. Primary antibody was diluted 1:2,000, and the blot was incubated at 4 °C overnight. The membrane was then washed with tris-buffered saline-Tween 20 (TBS-T) at RT and secondary antibody, diluted, 1:5,000 rate, and incubated at RT for 1 h. After washing with TBS-T, the image was developed by ECL Western Blotting Substrate (Pierce).

Subunit Profiling of *M. smegmatis*. For liquid culture, *M. smegmatis* strain was grown on Middlebrook 7H9 medium till OD_{600nm} ≈ 1 and collected by centrifuge at 4,500 × *g*, 4 °C for 20 min. For plates, wild-type *M. smegmatis* strain and ΔARP strain were plated on 7H10 plate or 7H10 plate supplied with 10 μM TPEN, and bacteria were collected by scraping. The bacterial pellet was washed and resuspended with polysome buffer (50 mM Tris-actate pH = 7.2, 12 mM $MgCl_2$, 50 mM NH_4Cl). Bacteria were pulverized by beads beating or French Press, and the lysate was centrifuged at 18,500 × *g*, 4 °C for 45 min. Cleared lysate was further loaded to a linear sucrose gradient (10 to 50%) at Beckman SW41 rotor and centrifuged at 39,000 rpm, 4 °C for 5 h. Gradients were fractioned with continuous A_{260} measurement, and fractions were collected for downstream analysis.

Relative Translation Rate Assay. The reporter used in this assay is depicted in *SI Appendix*, Fig. S9*A*. Of note is that the lysine and threonine codon in the Nluc sequence were codon-optimized to be neutral with regards to codon occupancy by AltRibo or CanRibo generated from prior ribosome profiling data, to minimize the bias in the assay. The codon-optimized Nluc was cloned to pMC1S vector with a C terminus tag to target Nluc from protease degradation (74). This would limit expression from the promoter in the absence of inducer to below detection limits, and therefore only newly synthesized protein upon addition of inducer would be measured by Nluc activity. Bacteria containing the reporter was grown in Sauton's medium to stationary phase (OD > 3) and diluted to OD ≈ 0.2 into Sauton's medium supplied with either 10 μM zinc sulfate or 0.5 μM TPEN, and ATc was added to the culture at a final concentration of 50 ng/mL. Five minutes after induction, bacteria were pelleted, washed twice, and resuspended in fresh medium as before but without ATc, and ± 200 μg/mL chloramphenicol as a protein synthesis inhibitor. Bacterial aliquots were collected every 10 min and fast frozen in liquid nitrogen. After samples from all time points were collected, luminescence was measured. For each condition, three biological replicates were included.

Ribosomal Decoding Assay. The procedure of dual luciferase-based mistranslation assay was carried out as previous described (51, 53). Briefly, the bacterial strains containing the reporter plasmid were grown to late stationary phase (OD > 3) and diluted to OD ≈ 0.2 into Sauton's medium supplied with either 10 μM zinc sulfate or 0.5 μM TPEN, following acetamide induction for 6 h. After induction, bacterial pellets were collected, and supernatant was discarded. Bacteria were disrupted by passive lysis buffer provided by dual luciferase kit (Promega), and Firefly and Renilla luminescence was measured by luminometer with 1,000 ms as integration time. For each experiment, three biological replicates were included.

Selective Ribosome Profiling with Affinity-Purified Tagged AltRibosomes. Bacterial cultures of dual-tagged strain A or strain B were grown until $OD600_{nm}$ ≈ 1 and treated with 100 μg/mL chloramphenicol for 3 min to arrest elongating ribosome before harvesting bacteria. Bacterial pellets were collect by centrifuging at 4,500 × *g*, 4 °C for 10 min. The pellet was washed and resuspended with ice-cold polysome buffer with minor recipe change (50 mM Tris-actate pH= 7.2, 12 mM MgCl2, 50 mM NH_4Cl, 10 mM $CaCl_2$, and 100 μg/mL chloramphenicol). The suspended bacterial suspension was dropped into liquid nitrogen and smashed into powder. The powder was smashed several times with repeated chilling with liquid nitrogen and was further pulverized with beads beating four to five times with chilling in liquid nitrogen between each step. After centrifugation at 18,500 × *g* for 45 min, the cleared lysate was transferred to a new tube supplied with 70 U/mL MNase to digest ribosome-unprotected mRNA. The predigested lysate was laid over a 1-M sucrose cushion and centrifuged at 30,000 rpm, 4 °C for 20 h in Beckman 70Ti rotor. After ultracentrifugation, the ribosome pellet was washed and dissolved in polysome buffer. The dissolved ribosome solution was further digested with MNase at 4 °C for 1 h. The digested ribosome fraction was incubated with either Flag resin or HA resin at 4 °C overnight. After washing of the bound resin, the resin was eluted with 3xFlag/3xHA peptide to isolate the AltRibo (eluate), and the remaining flow-through was confirmed as consisting almost entirely of CanRibos.

The procedure for building deep sequencing libraries was followed as previously described (43), with minor changes. The detailed protocol is described below. Ribosome-protected mRNA fragments were extracted by miRNeasy kit according to the manufacturer's instructions and size-selected for 26- to 34-nt fragment by marker oligo through 15% TBE-UREA (tris-borate ethylenediaminetetraacetic acid) PAGE. The corresponding region was sliced and smashed into pieces and soaked in 400 μL of RNA gel extraction buffer (300 mM sodium acetate pH 5.5, 1 mM EDTA (ethylenediaminetetraacetic acid), and 0.25% SDS) and rotated at RT overnight. RNA was precipitated with 1.5 μL of GlycoBlue and 500 μL of isopropanol. The RNA was dephosphorylated with 1 μL of T4 PNK at 37 °C for 1 h. RNA was extracted by isopropanol precipitation. Samples were then ligated with 0.5 μL of Universal miRNA cloning linker and 1.0 μL of T4 RNA ligase (truncated) at RT overnight. The ligation product was purified by isopropanol precipitation and visualized by 15% TBE-UREA PAGE. After slicing the corresponding ligated mRNA fragment, the samples were then subjected to reverse transcription with supersciptase III and RT-Primer. After incubating the reaction at 48 °C, 30 min, the RNA template was further hydrolyzed with 2 μL of 1 M NaOH at 98 °C for 20 min. The RT product was precipitated with isopropanol and size-selected with 15% TBE-UREA PAGE. The corresponding region was sliced and soaked in 400 μL of DNA gel extraction (300 mM NaCl, 10 mM Tris pH = 8, and 1 mM EDTA) and rotated at RT overnight. The complementary DNA (cDNA) was purified by isopropanol precipitation and circularized with 1 μL of CircLigase and incubated at 60 °C for 1 h. The circularized cDNA template was incubated with 1 μL of 10 mM Biotinylated rRNA subtraction oligo pool mix. The Oligo sequence was adopted from another study (44), with additional oligos newly designed according to our preliminary ribosome profiling data (*SI Appendix*, Table S2). The mixture was denatured for 90 s at 100 °C and then annealed at 0.1 °C/s to 37 °C. This was then incubated at 37 °C for 15 min. Thirty microliters of streptavidin C1 DynaBeads was added to the mixture and incubated for 15 min at 37 °C with mixing at 1,000 rpm. Then the mixture was placed on a magnetic rack to isolate the beads, the supernatant was transferred to a new tube, and cDNA was purified by isopropanol precipitation. The subsequent cDNA template was used for library amplification with Phusion high-fidelity DNA polymerase for 12 to 14 cycles. PCR products were purified from 8% TBE PAGE gel. The corresponding bands were sliced and soaked in DNA gel extraction buffer and rotated at RT overnight. The PCR products were purified by isopropanol precipitation, and the concentration and quality were measured with Agilent 2100 Bioanalyzer. Libraries were sequenced on the Illumina X-ten sequencer.

Semiquantitative Mass Spectrometry. Strain A was grown in Sauton's medium supplemented with 10 μM Zinc sulfate to OD_{600nm} ≈ 1, and bacterial pellets were collected by centrifugation at 4,500 × *g* for 20 min, 4 °C. For semiquantitative mass spectrometry, three biological replicates were collected and mixed together for further analysis. Total ribosome, CanRibo, and AltRibo were collected by using the same purification strategy described above for ribosome profiling. Western blot performed on samples confirmed the purity of each ribosome fraction. The purified ribosomes representing total ribosomes, AltRibos, and CanRibos were then subjected to mass spectrometry by TMTs as previously described (75) using a Thermo Scientific Q Exactive HF-X Hybrid Quadrupole-Orbitrap Mass Spectrometer.

Large-Scale Tagged Ribosome Purification for Biochemical Analysis. Bacterial cultures (~30 L) were grown to around OD_{600nm} ≈ 1, and bacterial pellets were collected by centrifugation at 4,500 × *g* for 20 min, 4 °C. Pellet was washed and resuspended in polysome buffer. Bacteria were disrupted by

French Press and centrifuged at 18,500 × *g*, 4 °C for 1 h to collect supernatant. MNase was added to the cleared lysate at a concentration of 70 U/mL and digested at 4 °C overnight. The digested lysate was loaded onto 1-M sucrose cushions and centrifuged at 30,000 rpm, 4 °C for 20 h. After centrifugation, the supernatant was discarded, and the ribosome pellet was washed with polysome buffer and dissolved in polysome buffer with gentle shaking at 4 °C. The crude ribosome suspension was further digested with MNase at 4 °C overnight. After secondary digestion, the ribosome preparation was dialyzed against Hepes:Polymix buffer (76, 77). The ribosome preparation was incubated with anti-Flag M2 beads at 4 °C overnight. After binding with M2 beads, the flow-through was collected as CanRibo and AltRibo was collected by eluting with Flag peptide. Each fraction, comprising total Ribo, CanRibo (flow-through), and AltRibo (Eluate), was probed by Western blotting for quality check and purity prior to further analysis.

In Vitro 70S Initiation Complex Formation. Initiation complex was formed by incubating 70S ribosome variants as described above (0.2 μM), [^{3}H]fMet-tRNA^{fMet} (0.5 μM), XR7mRNA (AUG-UAA) (78) (0.5 μM), initiation factors (0.5 μM) and guanosine triphosphate (GTP) (1 mM) at 37 °C for 15 min in Hepes:Polymix buffer (76). The reactions were thereafter filtered through BA-85 nitrocellulose membranes and washed with 10 mL of ice-cold Hepes:Polymix buffer (pH 7.5). The radioactivity retained on the filter was measured in a Beckman LC6500 scintillation counter.

In Vitro Initiator tRNA Binding. BODIPY-labeled Met-tRNA^{fMet} (0.1 μM) was rapidly mixed in stopped flow with 70S ribosomes (1 μM) preincubated with XR7mRNA (AUG-UAA) (0.5 μM). BODIPY fluorescence was excited at 575 nm, and the change in fluorescence signal was monitored in real time after passing through a 590-nm cutoff filter. The time course data were obtained by averaging three to five individual traces and fitted with single exponential model.

In Vitro Dipeptide Assay. For Met-Leu dipeptide formation, an initiation complex was formed with mycobacterial 70S ribosome variants (1 μM to 5 μM), AUG-CUG-UAA XR7 mRNA (20 μM) and [^{3}H]fMet-tRNA^{fMet} (1 μM), initiation factors (2 μM) at 37 °C. In parallel, an elongation mix was prepared which contained *M. smegmatis* EF-Tu (20 μM), EF-Ts (20 μM), tRNA^{Leu} (100 μM), Leu amino acid (0.5 mM), Leu-tRNA synthetase (1 unit per μL), and GTP (1 mM) at 37 °C. Both initiation complex and elongation mix containing energy pump adenosine 5′-triphosphate (1 mM), phosphoenolpyruvate (10 mM), pyruvate kinase, and myokinase (Sigma). The reaction was started by mixing equal volumes of the initiation complex and elongation complex at 37 °C and was quenched after 10 s by adding 17% formic acid. The peptides were isolated from the ribosome complex by KOH treatment and further analyzed by high-performance liquid chromatography (HPLC) equipped with a radioactivity detector.

Read Preparation and Alignment. The *M. smegmatis* mc^2-155 reference genome assembly (ASM1500v1) downloaded from Ensembl Bacteria Release 32 (https://bacteria.ensembl.org/index.html) was used for all analyses. For RNA sequencing (RNAseq), we performed quality control and trimmed adaptors using the FastQC and FASTX-Toolkit. For ribosome profiling, after quality control and adaptor removal, reads less than 25 nt long were discarded and longer than 36 nt were trimmed to 36 nt. Next, ribosome profile and RNAseq reads that aligned to rRNA and tRNA were removed using bowtie2 (79). We aligned the remaining reads to the genome using bowtie2 with "sensitive-local" option. The mapped reads were normalized to reads per kilobase million (RPKM) using total number of mapped reads.

A-Site Assignment. For each read, the A-site's position was inferred by taking the first nucleotide that was 12 nt upstream of the 3′ end of the read (80). Based on this, we generated a signal track of A-sites for all transcripts. ORFs that had been annotated in the reference were denoted as annotated ORFs (aORFs).

Polarization of Aligned Ribosome Profile Reads. The polarity score was calculated on the basis of aligned A-site signal track by adapting a previous method (45). The observed polarized reads from AltRibos were not due to ambiguous artifacts that might be caused by peaks around the start/stop codons, since the same result was observed whether or not the first and last 15 nt of the coding region were included in the analysis. The aORFs with more than 50 reads in coding sequences were plotted. In this study, we calculated the polarity score under AltRibo, CanRibo, and total ribosome population. Here we defined the concept of polarity shift by taking total ribosomes as the background input and subtracting the polarity score of background from the score of AltRibo-enriched/CanRibo-enriched populations.

Differential Ribosome Codon Reading. The calculation of codon occupancy was adapted from a previous method (46). For each aORF, only in-frame ribosome profiling fragments (RPFs) were included to study the frequencies of all codons. For each coding gene, its codon density was calculated by normalizing the observed RPF frequencies by the total frequencies of codons. Later, we included genes with at least 100 RPFs as input and obtained an averaged codon density for each codon. Here we denoted T_{codon_i} as the averaged codon occupancy of codon$_i$ for AltRibo or CanRibo population, while R_{codon_i} is the averaged codon occupancy of codon$_i$ for reference population, in this case, the total ribosomes. To better clarify the difference between AltRibo and CanRibo population, we further defined codon occupancy shift as follows:

$$\text{codon occupancy shift}_{\text{codon}_i} = \left(T_{\text{codon}_i} - R_{\text{codon}_i}\right)/R_{\text{codon}_i}.$$

Significantly different codon usage was detected by comparing the codon density of all studied aORFs under test conditions (AltRibo/CanRibo) against the corresponding density under the reference condition (total ribosome input) (*t* test *P* value < 0.05 and shift > 0.05 or shift < −0.05).

Additionaly, for each individual aORF, we correlated its codon density from AltRibo/CanRibo population with that from total ribosome population (Pearson correlation was used in this study).

Differential Codon Abundance. In this study, we used the concept of codon abundance to measure the occurrence of specific codons in the 50 codons within the 5′ or 3′ of the coding region. The calculation of codon abundance followed a previous study (81). To better demonstrate the difference, the final results were presented in the following form:

$$\text{Slope}_{codon_i} = \frac{\text{codon abundance}_{\text{codon}_i,3'} - \text{codon abundance}_{\text{codon}_i,5'}}{codon\ abundance_{\text{codon}_i,5'}}.$$

Slope$_{codon_i}$ represents the slope of *codon*$_i$ in which codon abundance$_{\text{codon}_i,3'}$ represents the codon abundance of *codon*$_i$ in the 3′ region, while codon abundance$_{\text{codon}_i,5'}$ represents the codon abundance of *codon*$_i$ in the 5′ region.

Differential Translation Analysis. Since AltRibo, CanRibo, and total ribosomes were collected from the same population of bacteria, to identify differential translated genes, we used edgeR on the corresponding ribosome profiling datasets (82). During analysis, replicates were included. Differentially translated genes were identified by $\log_2$ fold change (FC) > 0.5 (up-regulated) or $\log_2$ FC < −0.5 (down-regulated) and *P* value < 0.05. In this study, the datasets of total ribosome were treated as the control and compared against AltRibo or CanRibo to identify differentially translated genes.

Statistical Analysis. Appropriate statistical tests are detailed within each protocol and in the figure legends.

Data Availability. Ribosome profiling and RNAseq data presented in this study are available with GEO accession number GSE127827.

ACKNOWLEDGMENTS. We thank Jianhuo Fang from the Tsinghua genomic and synthetic biology core for help in preparing the ribosome profile libraries. We thank Eric Rubin and Hesper Rego for reading and commenting on the draft manuscript. This work was, in part, funded by grants from the Bill and Melinda Gates Foundation (Grant OPP1109789) and from the National Natural Science Foundation of China (Grant 31570129) and start-up funds from Tsinghua University to B.J. and from grants to S.S. from the Swedish Research Council (Grants 2018-05498 and 2016-06264) and Carl Tryggers Foundation (Grants CTS 18:338 and CTS 19:806). B.J. is an Investigator of the Wellcome Trust (207487/C/17/Z).

1. M. V. Rodnina, Translation in prokaryotes. *Cold Spring Harb. Perspect. Biol.* **10**, a032664 (2018).
2. V. Ramakrishnan, The ribosome emerges from a black box. *Cell* **159**, 979–984 (2014).
3. A. Jobe, Z. Liu, C. Gutierrez-Vargas, J. Frank, New insights into ribosome structure and function. *Cold Spring Harb. Perspect. Biol.* **11**, a032615 (2019).
4. F. H. Crick, On protein synthesis. *Symp. Soc. Exp. Biol.* **12**, 138–163 (1958).
5. S. Brenner, F. Jacob, M. Meselson, An unstable intermediate carrying information from genes to ribosomes for protein synthesis. *Nature* **190**, 576–581 (1961).
6. P. B. Moore, R. R. Traut, H. Noller, P. Pearson, H. Delius, Ribosomal proteins of *Escherichia coli*. II. Proteins from the 30 s subunit. *J. Mol. Biol.* **31**, 441–461 (1968).

7. E. Deusser, H. G. Wittmann, Ribosomal proteins: Variation of the protein composition in *Escherichia coli* ribosomes as function of growth rate. *Nature* **238**, 269–270 (1972).
8. J. Parenteau *et al*., Preservation of gene duplication increases the regulatory spectrum of ribosomal protein genes and enhances growth under stress. *Cell Rep.* **13**, 2516–2526 (2015).
9. N. R. Genuth, M. Barna, Heterogeneity and specialized functions of translation machinery: From genes to organisms. *Nat. Rev. Genet.* **19**, 431–452 (2018).
10. N. R. Genuth, M. Barna, The discovery of ribosome heterogeneity and its implications for gene regulation and organismal life. *Mol. Cell* **71**, 364–374 (2018).
11. J. E. Gerst, Pimp my ribosome: Ribosomal protein paralogs specify translational control. *Trends Genet.* **34**, 832–845 (2018).
12. M. B. Ferretti, K. Karbstein, Does functional specialization of ribosomes really exist? *RNA* **25**, 521–538 (2019).
13. E. W. Mills, R. Green, Ribosomopathies: There's strength in numbers. *Science* **358**, eaan2755 (2017).
14. Z. Shi *et al*., Heterogeneous ribosomes preferentially translate distinct subpools of mRNAs genome-wide. *Mol. Cell.* **67**, 71–83 e7 (2017).
15. Y. Zhang *et al*., Control of hematopoietic stem cell emergence by antagonistic functions of ribosomal protein paralogs. *Dev. Cell* **24**, 411–425 (2013).
16. N. Kondrashov *et al*., Ribosome-mediated specificity in Hox mRNA translation and vertebrate tissue patterning. *Cell* **145**, 383–397 (2011).
17. A. J. Warren, Molecular basis of the human ribosomopathy Shwachman-Diamond syndrome. *Adv. Biol. Regul.* **67**, 109–127 (2018).
18. K. Byrgazov, O. Vesper, I. Moll, Ribosome heterogeneity: Another level of complexity in bacterial translation regulation. *Curr. Opin. Microbiol.* **16**, 133–139 (2013).
19. M. van de Waterbeemd *et al*., High-fidelity mass analysis unveils heterogeneity in intact ribosomal particles. *Nat. Methods* **14**, 283–286 (2017).
20. A. C. Kaberdina, W. Szaflarski, K. H. Nierhaus, I. Moll, An unexpected type of ribosomes induced by kasugamycin: A look into ancestral times of protein synthesis? *Mol. Cell* **33**, 227–236 (2009).
21. O. Vesper *et al*., Selective translation of leaderless mRNAs by specialized ribosomes generated by MazF in *Escherichia coli*. *Cell* **147**, 147–157 (2011).
22. S. Chaudhuri *et al*., Kasugamycin potentiates rifampicin and limits emergence of resistance in *Mycobacterium tuberculosis* by specifically decreasing mycobacterial mistranslation. *eLife* **7**, 7 (2018).
23. P. H. Culviner, M. T. Laub, Global analysis of the *E. coli* toxin MazF reveals widespread cleavage of mRNA and the inhibition of rRNA maturation and ribosome biogenesis. *Mol. Cell* **70**, 868–880.e10 (2018).
24. C. Lange *et al*., Effects of kasugamycin on the translatome of *Escherichia coli*. *PLoS One* **12**, e0168143 (2017).
25. T. Mets *et al*., Fragmentation of *Escherichia coli* mRNA by MazF and MqsR. *Biochimie* **156**, 79–91 (2019).
26. C. M. Kurylo *et al*., Endogenous rRNA sequence variation can regulate stress response gene expression and phenotype. *Cell Rep.* **25**, 236–248 e6 (2018).
27. M. M. Parks *et al*., Variant ribosomal RNA alleles are conserved and exhibit tissue-specific expression. *Sci. Adv.* **4**, eaao0665 (2018).
28. J. D. Dinman, Pathways to specialized ribosomes: The brussels lecture. *J. Mol. Biol.* **428**, 2186–2194 (2016).
29. E. Emmott, M. Jovanovic, N. Slavov, Ribosome stoichiometry: From form to function. *Trends Biochem. Sci.* **44**, 95–109 (2019).
30. N. Yutin, P. Puigbò, E. V. Koonin, Y. I. Wolf, Phylogenomics of prokaryotic ribosomal proteins. *PLoS One* **7**, e36972 (2012).
31. K. S. Makarova, V. A. Ponomarev, E. V. Koonin, Two C or not two C: Recurrent disruption of Zn-ribbons, gene duplication, lineage-specific gene loss, and horizontal gene transfer in evolution of bacterial ribosomal proteins. *Genome Biol.* **2**, research0033 (2001).
32. S. Prisic *et al*., Zinc regulates a switch between primary and alternative S18 ribosomal proteins in *Mycobacterium tuberculosis*. *Mol. Microbiol.* **97**, 263–280 (2015).
33. V. Tobiasson, A. Dow, S. Prisic, A. Amunts, Zinc depletion does not necessarily induce ribosome hibernation in mycobacteria. *Proc. Natl. Acad. Sci. U.S.A.* **116**, 2395–2397 (2019).
34. A. Gaballa, T. Wang, R. W. Ye, J. D. Helmann, Functional analysis of the *Bacillus subtilis* Zur regulon. *J. Bacteriol.* **184**, 6508–6514 (2002).
35. S. E. Gabriel, J. D. Helmann, Contributions of Zur-controlled ribosomal proteins to growth under zinc starvation conditions. *J. Bacteriol.* **191**, 6116–6122 (2009).
36. H. Nanamiya *et al*., Zinc is a key factor in controlling alternation of two types of L31 protein in the *Bacillus subtilis* ribosome. *Mol. Microbiol.* **52**, 273–283 (2004).
37. G. Akanuma, H. Nanamiya, Y. Natori, N. Nomura, F. Kawamura, Liberation of zinc-containing L31 (RpmE) from ribosomes by its paralogous gene product, YtiA, in *Bacillus subtilis*. *J. Bacteriol.* **188**, 2715–2720 (2006).
38. Y. Li *et al*., Zinc depletion induces ribosome hibernation in mycobacteria. *Proc. Natl. Acad. Sci. U.S.A.* **115**, 8191–8196 (2018).
39. Z. Li *et al*., Cryo-EM structure of *Mycobacterium smegmatis* ribosome reveals two unidentified ribosomal proteins close to the functional centers. *Protein Cell* **9**, 384–388 (2018).
40. A. H. Becker, E. Oh, J. S. Weissman, G. Kramer, B. Bukau, Selective ribosome profiling as a tool for studying the interaction of chaperones and targeting factors with nascent polypeptide chains and ribosomes. *Nat. Protoc.* **8**, 2212–2239 (2013).
41. E. Oh *et al*., Selective ribosome profiling reveals the cotranslational chaperone action of trigger factor in vivo. *Cell* **147**, 1295–1308 (2011).
42. S. Elgamal *et al*., EF-P dependent pauses integrate proximal and distal signals during translation. *PLoS Genet.* **10**, e1004553 (2014).
43. N. T. Ingolia, G. A. Brar, S. Rouskin, A. M. McGeachy, J. S. Weissman, The ribosome profiling strategy for monitoring translation in vivo by deep sequencing of ribosome-protected mRNA fragments. *Nat. Protoc.* **7**, 1534–1550 (2012).
44. S. S. Shell *et al*., Leaderless transcripts and small proteins are common features of the mycobacterial translational landscape. *PLoS Genet.* **11**, e1005641 (2015).
45. A. P. Schuller, C. C. Wu, T. E. Dever, A. R. Buskirk, R. Green, eIF5A functions globally in translation elongation and termination. *Mol. Cell* **66**, 194–205.e5 (2017).
46. F. Loayza-Puch *et al*., Tumour-specific proline vulnerability uncovered by differential ribosome codon reading. *Nature* **530**, 490–494 (2016).
47. D. D. Nedialkova, S. A. Leidel, Optimization of codon translation rates via tRNA modifications maintains proteome integrity. *Cell* **161**, 1606–1618 (2015).
48. E. M. Novoa, M. Pavon-Eternod, T. Pan, L. Ribas de Pouplana, A role for tRNA modifications in genome structure and codon usage. *Cell* **149**, 202–213 (2012).
49. J. B. Andersen *et al*., New unstable variants of green fluorescent protein for studies of transient gene expression in bacteria. *Appl. Environ. Microbiol.* **64**, 2240–2246 (1998).
50. O. Kurkcuoglu, P. Doruker, T. Z. Sen, A. Kloczkowski, R. L. Jernigan, The ribosome structure controls and directs mRNA entry, translocation and exit dynamics. *Phys. Biol.* **5**, 46005 (2008).
51. Y. X. Chen, M. Pan, Y. M. Chen, B. Javid, Measurement of specific mycobacterial mistranslation rates with gain-of-function reporter systems. *J. Vis. Exp.* **26**, 146 (2019).
52. B. Javid *et al*., Mycobacterial mistranslation is necessary and sufficient for rifampicin phenotypic resistance. *Proc. Natl. Acad. Sci. U.S.A.* **111**, 1132–1137 (2014).
53. T. Leng, M. Pan, X. Xu, B. Javid, Translational misreading in *Mycobacterium smegmatis* increases in stationary phase. *Tuberculosis (Edinb.)* **95**, 678–681 (2015).
54. M. S. Siegrist *et al*., Mycobacterial Esx-3 is required for mycobactin-mediated iron acquisition. *Proc. Natl. Acad. Sci. U.S.A.* **106**, 18792–18797 (2009).
55. A. Serafini, F. Boldrin, G. Palù, R. Manganelli, Characterization of a *Mycobacterium tuberculosis* ESX-3 conditional mutant: Essentiality and rescue by iron and zinc. *J. Bacteriol.* **191**, 6340–6344 (2009).
56. W. Song *et al*., Divergent rRNAs as regulators of gene expression at the ribosome level. *Nat. Microbiol.* **4**, 515–526 (2019).
57. N. Segev, J. E. Gerst, Specialized ribosomes and specific ribosomal protein paralogs control translation of mitochondrial proteins. *J. Cell Biol.* **217**, 117–126 (2018).
58. H. S. Zaher, R. Green, Hyperaccurate and error-prone ribosomes exploit distinct mechanisms during tRNA selection. *Mol. Cell* **39**, 110–120 (2010).
59. A. B. Loveland, A. A. Korostelev, Structural dynamics of protein S1 on the 70S ribosome visualized by ensemble cryo-EM. *Methods* **137**, 55–66 (2018).
60. T. Cortes *et al*., Genome-wide mapping of transcriptional start sites defines an extensive leaderless transcriptome in *Mycobacterium tuberculosis*. *Cell Rep.* **5**, 1121–1131 (2013).
61. E. B. Sawyer, A. D. Grabowska, T. Cortes, Translational regulation in mycobacteria and its implications for pathogenicity. *Nucleic Acids Res.* **46**, 6950–6961 (2018).
62. J. Hentschel *et al*., The complete structure of the *Mycobacterium smegmatis* 70S ribosome. *Cell Rep.* **20**, 149–160 (2017).
63. K. Yang *et al*., Structural insights into species-specific features of the ribosome from the human pathogen *Mycobacterium tuberculosis*. *Nucleic Acids Res.* **45**, 10884–10894 (2017).
64. Y. Li *et al*., Reply to Tobiasson et al.: Zinc depletion is a specific signal for induction of ribosome hibernation in mycobacteria. *Proc. Natl. Acad. Sci. U.S.A.* **116**, 2398–2399 (2019).
65. H. Gao, W. Dai, L. Zhao, J. Min, F. Wang, The role of zinc and zinc homeostasis in macrophage function. *J. Immunol. Res.* **2018**, 6872621 (2018).
66. S. Mishra, T. Ahmed, A. Tyagi, J. Shi, S. Bhushan, Structures of *Mycobacterium smegmatis* 70S ribosomes in complex with HPF, tmRNA, and P-tRNA. *Sci. Rep.* **8**, 13587 (2018).
67. A. Trauner, K. E. Lougheed, M. H. Bennett, S. M. Hingley-Wilson, H. D. Williams, The dormancy regulator DosR controls ribosome stability in hypoxic mycobacteria. *J. Biol. Chem.* **287**, 24053–24063 (2012).
68. E. M. Novoa, L. Ribas de Pouplana, Speeding with control: Codon usage, tRNAs, and ribosomes. *Trends Genet.* **28**, 574–581 (2012).
69. S. Marzi *et al*., Structured mRNAs regulate translation initiation by binding to the platform of the ribosome. *Cell* **130**, 1019–1031 (2007).
70. A. Dow, S. Prisic, Alternative ribosomal proteins are required for growth and morphogenesis of *Mycobacterium smegmatis* under zinc limiting conditions. *PLoS One* **13**, e0196300 (2018).
71. S. B. Snapper, R. E. Melton, S. Mustafa, T. Kieser, W. R. Jacobs Jr., Isolation and characterization of efficient plasmid transformation mutants of *Mycobacterium smegmatis*. *Mol. Microbiol.* **4**, 1911–1919 (1990).
72. H. W. Su *et al*., The essential mycobacterial amidotransferase GatCAB is a modulator of specific translational fidelity. *Nat. Microbiol.* **1**, 16147 (2016).
73. K. C. Murphy, K. Papavinasasundaram, C. M. Sassetti, Mycobacterial recombineering. *Methods Mol. Biol.* **1285**, 177–199 (2015).
74. M. C. Blokpoel, R. O'Toole, M. J. Smeulders, H. D. Williams, Development and application of unstable GFP variants to kinetic studies of mycobacterial gene expression. *J. Microbiol. Methods* **54**, 203–211 (2003).
75. Y. W. Zhang *et al*., HspX promotes the polar localization of mycobacterial protein aggregates. *Sci. Rep.* **9**, 14571 (2019).
76. R. K. Koripella *et al*., A conserved histidine in switch-II of EF-G moderates release of inorganic phosphate. *Sci. Rep.* **5**, 12970 (2015).
77. C. S. Mandava *et al*., Bacterial ribosome requires multiple L12 dimers for efficient initiation and elongation of protein synthesis involving IF2 and EF-G. *Nucleic Acids Res.* **40**, 2054–2064 (2012).
78. D. V. Freistroffer, M. Y. Pavlov, J. MacDougall, R. H. Buckingham, M. Ehrenberg, Release factor RF3 in E.coli accelerates the dissociation of release factors RF1 and RF2 from the ribosome in a GTP-dependent manner. *EMBO J.* **16**, 4126–4133 (1997).
79. B. Langmead, S. L. Salzberg, Fast gapped-read alignment with Bowtie 2. *Nat. Methods* **9**, 357–359 (2012).
80. F. Mohammad, C. J. Woolstenhulme, R. Green, A. R. Buskirk, Clarifying the translational pausing landscape in bacteria by ribosome profiling. *Cell Rep.* **14**, 686–694 (2016).
81. Y. Nakamura, T. Gojobori, T. Ikemura, Codon usage tabulated from international DNA sequence databases: Status for the year 2000. *Nucleic Acids Res.* **28**, 292 (2000).
82. M. D. Robinson, D. J. McCarthy, G. K. Smyth, edgeR: A Bioconductor package for differential expression analysis of digital gene expression data. *Bioinformatics* **26**, 139–140 (2010).